

## Modulated Phase of an Ising System with Quinary and Binary Interactions on a Cayley Tree-like Lattice: Rectangular Chandelier

Selman Uğuz<sup>1,\*</sup> and Hasan Akin<sup>2,†</sup>

<sup>1</sup>*Harran University, Arts and Science Faculty,  
Department of Mathematics, Sanliurfa, 63120, Turkey*

<sup>2</sup>*Zirve University, Faculty of Education,  
Department of Mathematics, Gaziantep, 27260, Turkey*

(Received August 19, 2010)

In the present work we study the phase diagrams for the Ising model on a Cayley tree-like lattice, a new lattice type called a *Rectangular Chandelier*, with competing nearest-neighbor interactions  $J_1$ , prolonged next-nearest-neighbor interactions  $J_p$ , and one-level next-nearest-neighbor quinary interactions  $J_{l_1}^{(5)}$ . The diagrams contain some multicritical Lifshitz points that are at nonzero temperature and many modulated new phases. This appears to shift the multicritical Lifshitz point to finite temperature, while it was stuck at zero temperature  $T$  for all systems with competing interactions in the previous works. To perform this study, an iterative scheme similar to that appearing in real space renormalization group frameworks is established; it recovers, as a particular case, the previous work of the Vannimenus extension result given by Ganikhodjaev *et al.* for  $k = 4$ . At vanishing temperature, the phase diagram is fully determined for all values and signs of the parameters  $J_1$ ,  $J_p$ , and  $J_{l_1}^{(5)}$ . For some critical points, the variation of the wavevector with temperature in the modulated phase is also analyzed.

PACS numbers: 05.50.+q, 64.60.-i, 64.60.De

### I. INTRODUCTION

A phase diagram of a model with a variety of transition lines and modulated phases is obtained via the presence of competing interactions in magnetic and ferroelectric systems. The ANNNI (axial next-nearest-neighbor Ising) model, which consists of an Ising spin Hamiltonian on a Cayley tree with ferromagnetic interactions on the planes and competing ferromagnetic and antiferromagnetic interactions between nearest and next-nearest neighbors along an axial direction, is known to reproduce some features of these complex phase diagrams [1]. The Ising model on a Cayley tree of order  $k$  with competing interactions has recently been studied extensively because of the appearance of nontrivial magnetic orderings [2] (see also the references in [2]). Also, the Ising model has found some applications in physical, chemical, and biological systems, and even in sociology. The Cayley tree is not a realistic lattice; however, its amazing topology makes the exact calculation of various quantities possible. For many problems the solution on a tree is much simpler than on a regular lattice and is equivalent to the standard Bethe-Peierls theory [3]. In the literature, there have been works on many different lattice types similar to Cayley trees [4, 5]. In this

paper, we produce a Cayley tree-like lattice [4, 5], which we call a *Rectangular Chandelier* from the configuration model given in Fig. 1. As initiated by Vannimenus [2], a Cayley tree is a counterpart of the ANNNI model, which is used to provide an approximate description of some materials, such as CESb [6] and ferroelectric  $\text{NaNNO}_2$  [7]. In recent years, the investigation of phase diagrams of the Ising model has attracted increased attention. More complicated models have been studied on tree-like lattices, with the hope of discovering new phases or unusual types of behavior. The important point is that statistical mechanics on trees involves nonlinear recursion equations and is naturally connected to the rich world of dynamical systems, a world presently under intense investigation (see the references in [2, 4, 5]). As in the Cayley tree, one can consider two types of next-nearest-neighbors: prolonged and one-level next-nearest-neighbors on the Cayley tree-like lattice (for definitions see below). In the case of the Ising model on the Cayley tree of second order, i.e.,  $k = 2$ , with competing nearest-neighbor interactions  $J_1$  and prolonged next-nearest-neighbor interactions  $J_p$ , Vannimenus [2] was able to find new modulated phases, in addition to the expected paramagnetic and ferromagnetic ones. From this result it follows that the Ising model with competing interactions on a Cayley tree is of real interest, since it has many similarities with models on periodic lattices. In fact it has many common features with them, in particular the existence of a modulated phase, and shows no sign of pathological behavior, at least no more than mean-field theories of similar systems [2]. Inawashiro *et al.* [8, 9] independently of Vannimenus investigated the Ising model with nearest-neighbors and prolonged next-nearest-neighbor interactions on a Cayley tree, but they allowed  $J_p = J_o$ , where  $J_o$  is the one-level next-nearest-neighbor interaction on the Cayley tree of order two. Later Mariz *et al.* [10] extended this results assuming the existence also of a binary interaction  $J_o$  on a Cayley tree of order 2. Recently Ganikhodjaev *et al.* have obtained a general result of the Vannimenus work on a Cayley tree of arbitrary finite order  $k$  [11]. In a previous paper [12], we have constructed a Cayley tree-like lattice which we called a *Triangular Chandelier* from the similar configuration model given in Fig. 1. In [12], we have investigated the phase diagrams of an Ising model on a Triangular Chandelier with competing nearest-neighbors  $J_1$ , prolonged next-nearest-neighbors  $J_p$ , and one-level next-nearest-neighbors quadruple interactions  $J_{l_1}$ .

The aim of this paper is to extend the Vannimenus and Ganikhodjaev *et al.* [11] results to the Rectangular Chandelier (for the order  $k = 4$ ) by adding one-level next-nearest-neighbor quinary interactions  $J_{l_1}^{(5)}$ . We clarify the role of  $J_{l_1}^{(5)}$  with many interesting features similar to those given in the previous work (see [12] for the details). By using similar computational techniques as in [2, 10, 12], we describe the complex phase diagrams of an Ising model on a *Rectangular Chandelier* in the Hamiltonian 3-parameter space. For some given values of  $-J_p/J_1$  and  $J_{l_1}^{(5)}/J_1$ , we also present several interesting features at finite temperatures.

## II. PRELIMINARIES AND DEFINITIONS

*Cayley Tree and Rectangular Chandelier.* A Cayley tree  $\Gamma^k$  of order  $k \geq 1$  is an infinite

tree, i.e., a graph without cycles with exactly  $k + 1$  edges issuing from each vertex. Let us denote the Cayley tree as  $\Gamma^k = (V, \Lambda)$ , where  $V$  is the set of vertices of  $\Gamma^k$  and  $\Lambda$  is the set of edges of  $\Gamma^k$ . Two vertices  $x$  and  $y$  with  $x, y \in V$  are called *nearest-neighbors* if there exists an edge  $l \in \Lambda$  connecting them, which is denoted by  $l = \langle x, y \rangle$ . The distance  $d(x, y)$ ,  $x, y \in V$ , on the Cayley tree  $\Gamma^k$ , is the number of edges in the shortest path from  $x$  to  $y$ . For a fixed  $x_0 \in V$  we set  $W_n = \{x \in V | d(x, x_0) = n\}$ ,  $V_n = \{x \in V | d(x, x_0) \leq n\} = \bigcup_{i=0}^n W_i$ , and  $L_n$  denotes the set of edges in  $V_n$ . The fixed vertex  $x_0$  is called the 0-th level and the vertices in  $W_n$  are called the  $n$ -th level. For the sake of simplicity we put  $|x| = d(x, x_0)$ ,  $x \in V$ . Two vertices  $x, y \in V$  are called *the next-nearest-neighbors* if  $d(x, y) = 2$ . The next-nearest-neighbor vertices  $x$  and  $y$  are called *prolonged next-nearest-neighbors* if  $|x| \neq |y|$  and this is denoted by  $> \widetilde{x, y} <$ . The next-nearest-neighbor vertices  $x, y \in V$  that are not prolonged are called *one-level next-nearest-neighbors* since  $|x| = |y|$  and they are denoted by  $> x, y <$ . The vertices  $x, y, z, t$ , and  $w$  are called *one-level quinary next-nearest-neighbors* which is denoted by  $> x, y, \bar{z}, t, w <$ , if there is a vertex  $x$  such that  $\{x, y\}$ ,  $\{x, z\}$ ,  $\{x, t\}$  and  $\{x, w\}$  are nearest neighbors and  $\{y, z, t, w\}$  are situated on the same level. Below we will consider a semi-infinite Cayley tree-like (Rectangular Chandelier) lattice denoted by  $RC_+^k$  of  $k = 4$  order, i.e., an infinite graph without cycles with 7 edges issuing from each vertex except for  $x_0$  which has only 4 edges. In this work we use the same concepts and definitions for a Rectangular Chandelier as in a Cayley tree. We consider the set of all configurations on  $W_0 = \{x_0\}$  and  $W_1 = \{x_1, x_2, x_3, x_4\}$  with spin values respectively  $\{i_0\}$ ,  $\{i_0, i_1, i_2, i_3, i_4\}$  and generalize them as shown in Fig. 1. *The Model.* For the Ising model with spin values in  $\Phi = \{-1, 1\}$ , the relevant Hamiltonian with competing nearest-neighbor  $J_1$ , prolonged next-nearest-neighbor binary interactions  $J_p$ , and one-level next-nearest-neighbor quinary interactions  $J_{l_1}^{(5)}$  has the form

$$\begin{aligned}
 H(\sigma) &= -J_1 \sum_{\langle x, y \rangle} \sigma(x)\sigma(y) - J_p \sum_{> \widetilde{x, y} <} \sigma(x)\sigma(y) \\
 &\quad - J_{l_1}^{(5)} \sum_{> x, y, \bar{z}, t, w <} \sigma(x)\sigma(y)\sigma(z)\sigma(t)\sigma(w),
 \end{aligned} \tag{1}$$

where  $J_1, J_p, J_{l_1}^{(5)} \in R$  are coupling constants. In the presence of  $J_p$  with  $J_{l_1}^{(5)} = 0$  for  $k = 2$  this model was considered by Vannimenus [2]. He proved that the phase diagram contains a new modulated phase along with the expected paramagnetic and ferromagnetic ones. The case  $J_{l_1}^{(5)} = 0$  with binary interaction of  $J_o$  (see [10]) on a Cayley tree of order 2 was considered in [10]. Recently the model (1) on a Cayley tree of arbitrary order  $k$  with the case  $J_{l_1}^{(5)} = 0$  was studied in [11] as a Vannimenus extension result.

In this work we consider the model (1) on a new designed lattice model which we call a Rectangular Chandelier.

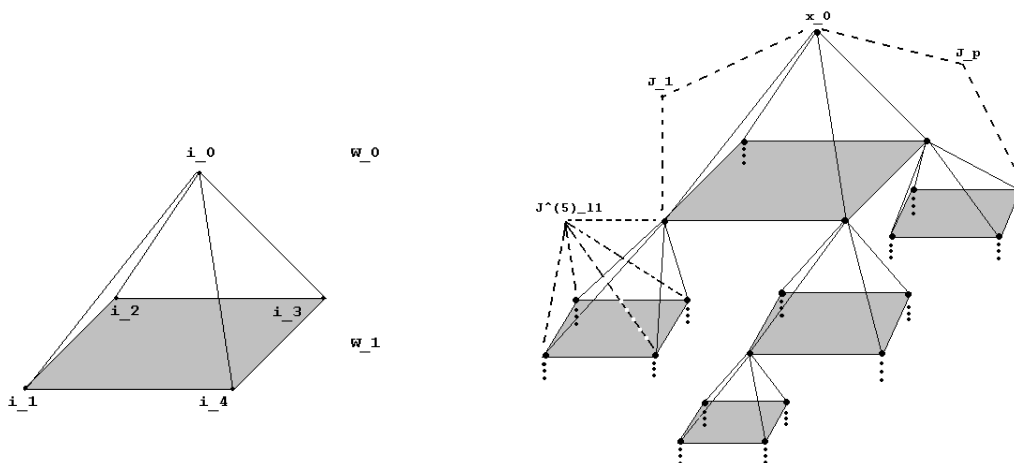


FIG. 1: *Left Figure:* The spin in the root  $x_0$  called the  $0$ th level is  $i_0$ .  $W_0$  and  $W_1$  of a triangular chandelier lattice consist of  $\{i_0\}$  and  $\{i_1, i_2, i_3, i_4\}$  respectively. *Right Figure:* A semi-infinite Cayley tree-like lattice: Rectangular Chandelier. The vertex  $x_0$  is the root of the lattice that emanates from the four edges. In the model (1) we have competing  $J_1$ ,  $J_p$ , and  $J_{l_1}^{(5)}$  interactions.

### III. RECURRENCE EQUATIONS

In order to produce the recurrence equations, we consider the relation of the partition function on  $V_n$  to the partition function on subsets of  $V_{n-1}$ . Given the initial conditions on  $V_1$ , the recurrence equations indicate how their influence propagates down the Rectangular Chandelier. Let  $Z^{(n)} \left( \begin{matrix} i_0 \\ i_1, i_2, i_3, i_4 \end{matrix} \right)$  be the partition function on  $V_n$  where the spin in the root  $x_0$  is  $i_0$  and the 3 spins in the proceeding ones are  $i_1, i_2, i_3, i_4$  (see Fig. 1). The partition function  $Z^{(n)}$  in volume  $V_n$  is defined by  $Z^{(n)} = \sum_{\sigma \in V_n} \exp(-\beta H(\sigma))$ , where  $\beta = 1/T$  is the inverse temperature. There are *a priori* 32 different  $Z^{(n)}$  to consider (following along the lines of Vannimenus work [2]). It is reasonable, though, to assume that the different branches are equivalent, as is usually done for models on trees. That is,  $Z^{(n)} \left( \begin{matrix} + \\ +, +, +, - \end{matrix} \right) = Z^{(n)} \left( \begin{matrix} + \\ +, +, -, + \end{matrix} \right) = \dots$ , etc. This implies that there are only 10

independent variables, namely

$$\begin{aligned}
 z_1 &= Z^{(n)} \begin{pmatrix} + \\ +, +, +, + \end{pmatrix}, & z_2 &= Z^{(n)} \begin{pmatrix} + \\ +, +, +, - \end{pmatrix}, \\
 z_3 &= Z^{(n)} \begin{pmatrix} + \\ +, +, -, - \end{pmatrix}, & z_4 &= Z^{(n)} \begin{pmatrix} + \\ +, -, -, - \end{pmatrix}, \\
 z_5 &= Z^{(n)} \begin{pmatrix} + \\ -, -, -, - \end{pmatrix}, & z_6 &= Z^{(n)} \begin{pmatrix} - \\ +, +, +, + \end{pmatrix}, \\
 z_7 &= Z^{(n)} \begin{pmatrix} - \\ +, +, +, - \end{pmatrix}, & z_8 &= Z^{(n)} \begin{pmatrix} - \\ +, +, -, - \end{pmatrix}, \\
 z_9 &= Z^{(n)} \begin{pmatrix} - \\ +, -, -, - \end{pmatrix}, & z_{10} &= Z^{(n)} \begin{pmatrix} - \\ -, -, -, - \end{pmatrix}.
 \end{aligned}$$

Then an arbitrary  $Z^{(n)} \begin{pmatrix} i_0 \\ i_1, i_2, i_3, i_4 \end{pmatrix}$  is written as a combination of  $z_1, z_2, z_3, \dots, z_{10}$ .

Primed variables  $(z'_1, z'_2, \dots)$  correspond to  $Z^{(n+1)}$ , and the interactions appear through the parameters  $a = \exp(J_1/T)$ ,  $b = \exp(J_p/T)$ ,  $c = \exp(J_{l_1}^{(5)}/T)$ . Hence the following equations can be obtained:

$$\begin{aligned}
 z'_1 &= a^4(b^4cz_1 + 4b^2c^{-1}z_2 + 6cz_3 + 4b^{-2}c^{-1}z_4 + b^{-4}cz_5)^4, \\
 z'_5 &= a^{-4}(b^4c^{-1}z_6 + 4b^2cz_7 + 6c^{-1}z_8 + 4b^{-2}cz_9 + b^{-4}c^{-1}z_{10})^4, \\
 z'_6 &= a^{-4}(b^{-4}cz_1 + 4b^{-2}c^{-1}z_2 + 6cz_3 + 4b^2c^{-1}z_4 + b^4cz_5)^4, \\
 z'_{10} &= a^4(b^{-4}c^{-1}z_6 + 4b^{-2}cz_7 + 6c^{-1}z_8 + 4b^2cz_9 + b^4c^{-1}z_{10})^4.
 \end{aligned}$$

In [12] it was briefly described how to obtain the above equations  $(z'_n)$ . For further details, we refer to [12]. It is important to note that  $z_2^4 = z_1^3 z_5$ ,  $z_3^4 = z_1^2 z_5^2$ ,  $z_4^4 = z_1 z_5^3$ ,  $z_7^4 = z_6^3 z_{10}$ ,  $z_8^4 = z_6^2 z_{10}^2$  and  $z_9^4 = z_6 z_{10}^3$ , so only four independent variables remain, and through the introduction of the new variables  $u_i = \sqrt[4]{z_i}$ , we produce the following recurrence system:  $u'_1 = a(b^4cu_1^4 + 4b^2c^{-1}u_1^3u_5 + 6cu_1^2u_5^2 + 4b^{-2}c^{-1}u_1u_5^3 + b^{-4}cu_5^4)$ ,  $u'_5 = a^{-1}(b^4c^{-1}u_6^4 + 4b^2cu_6^3u_{10} + 6c^{-1}u_6^2u_{10}^2 + 4b^{-2}cu_6u_{10}^3 + b^{-4}c^{-1}u_{10}^4)$ ,  $u'_6 = a^{-1}(b^{-4}cu_1^4 + 4b^{-2}c^{-1}u_1^3u_5 + 6cu_1^2u_5^2 + 4b^2c^{-1}u_1u_5^3 + b^4cu_5^4)$ ,  $u'_{10} = a(b^{-4}c^{-1}u_6^3 + 4b^{-2}cu_6^3u_{10} + 6c^{-1}u_6^2u_{10}^2 + 4b^2cu_6u_{10}^3 + b^4c^{-1}u_{10}^4)$ .

The total partition function  $Z^{(n)}$  is given in terms of  $(u_i)$  by  $Z^{(n)} = (u_1 + u_5)^4 + (u_6 + u_{10})^4$ . For a discussion of the phase diagrams, the following choice of reduced variables is convenient:

$$x = \frac{u_5 + u_6}{u_1 + u_{10}}, \quad y_1 = \frac{u_1 - u_{10}}{u_1 + u_{10}}, \quad y_2 = \frac{u_5 - u_6}{u_1 + u_{10}}. \tag{2}$$

The variable  $x$  is just a measure of the frustration of the nearest-neighbor bonds and is not an order parameter like  $y_1, y_2$ . Then the relations now have the following form:

$$x' = \frac{1}{a^2 D}(A_1 + A_2), \quad y'_1 = \frac{1}{D}(A_3 - A_4), \quad y'_2 = \frac{1}{a^2 D}(A_1 - A_2),$$

where

$$A_1 = b^4 c^{-1}(x - y_2)^4 + 4b^2 c(x - y_2)^3(1 - y_1) + 6c^{-1}(x - y_2)^2(1 - y_1)^2 + 4b^{-2}c(x - y_2)(1 - y_1)^3 + b^{-4}c^{-1}(1 - y_1)^4;$$

$$A_2 = b^{-4}c(1 + y_1)^4 + 4b^{-2}c^{-1}(1 + y_1)^3(x + y_2) + 6c(1 + y_1)^2(x + y_2)^2 + 4b^2c^{-1}(1 + y_1)(x + y_2)^3 + b^4c(x + y_2)^4;$$

$$A_3 = b^4c(1 + y_1)^4 + 4b^2c^{-1}(1 + y_1)^3(x + y_2) + 6c(1 + y_1)^2(x + y_2)^2 + 4b^{-2}c^{-1}(1 + y_1)(x + y_2)^3 + b^{-4}c(x + y_2)^4;$$

$$A_4 = b^{-4}c^{-1}(x - y_2)^4 + 4b^{-2}c(x - y_2)^3(1 - y_1) + 6c^{-1}(x - y_2)^2(1 - y_1)^2 + 4b^2c(x - y_2)(1 - y_1)^3 + b^{-4}c^{-1}(1 - y_1)^4;$$

$$D = A_3 + A_4.$$

The average magnetization  $m$  for the  $n$ th generation is defined by

$$m = \frac{(1 + x + y_1 + y_2)^4 - (1 + x - y_1 - y_2)^4}{(1 + x + y_1 + y_2)^4 + (1 + x - y_1 - y_2)^4}. \quad (3)$$

The systems of three equations finally obtained  $(x', y'_1, y'_2)$  is essentially more complicated than the similar basic equations of the Ising model [2], [12], and [10]. In the next section we use numerical methods to study its detailed behavior.

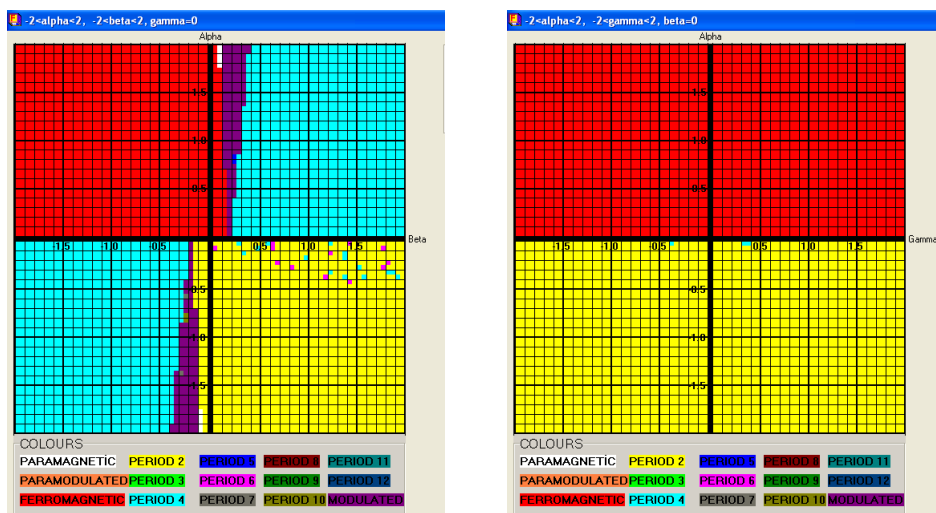
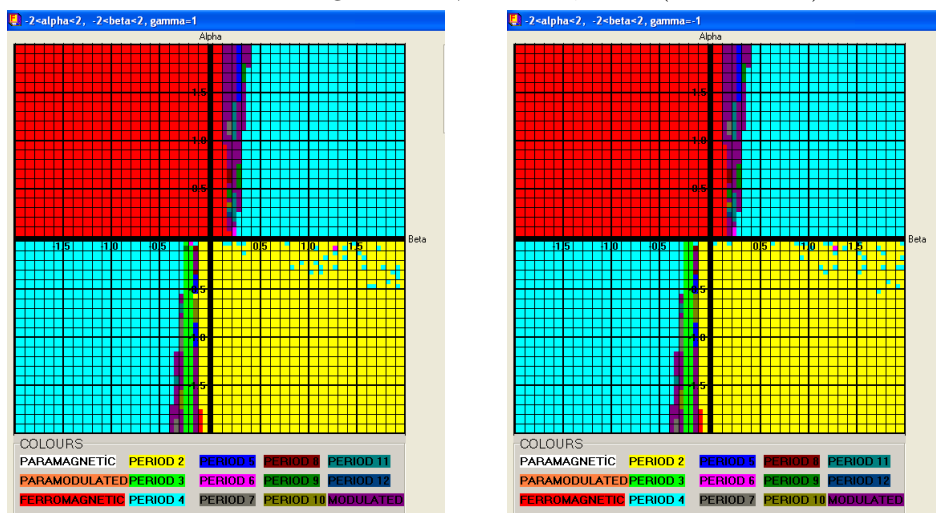
#### IV. THE PHASE DIAGRAMS IN THE HAMILTONIAN 3-PARAMETER SPACE

In this section we study the comprehensive behavior of the phase diagrams which are obtained by numerical methods. It is known that a phase diagram of a model describes a morphology of phases, transitions from one phase to another, stability of phases, and corresponding transition lines (see [2, 10, 13, 14] for the details).

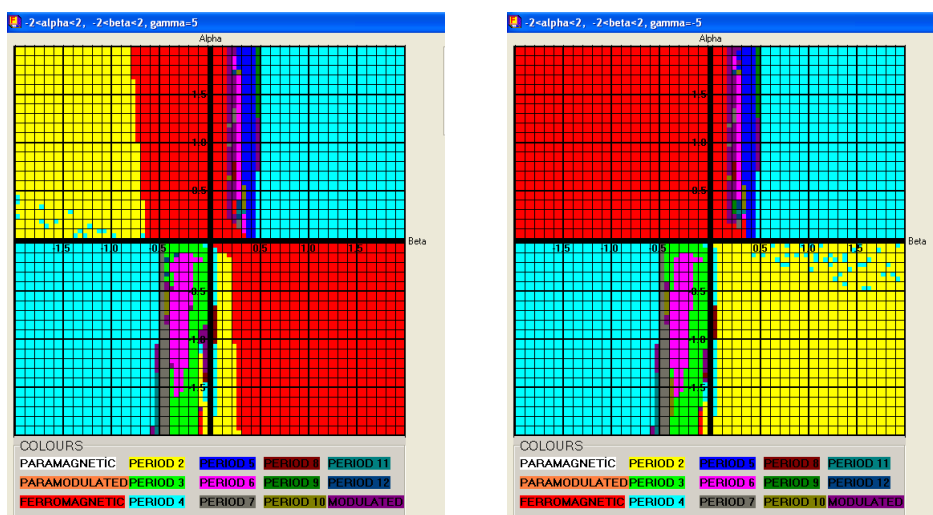
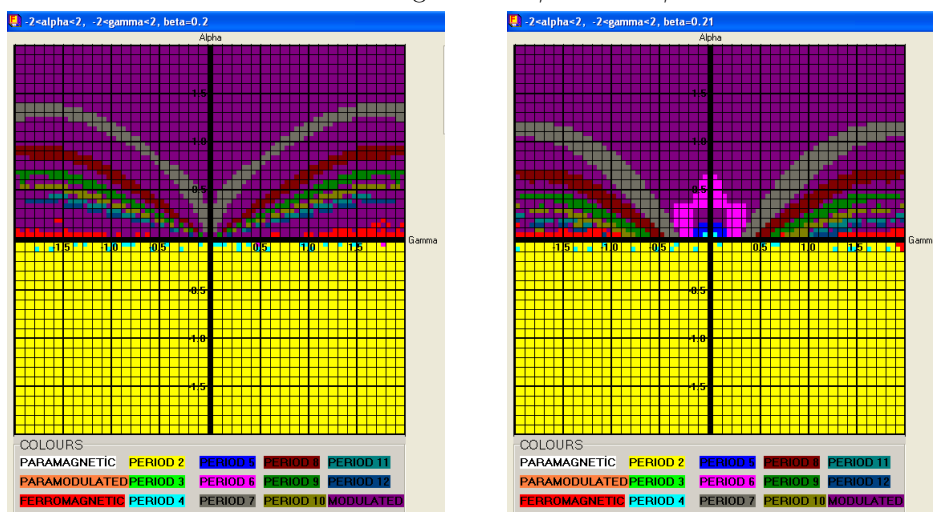
It is convenient to know the broad features of the phase diagram before discussing the different transitions in more detail. This can be achieved numerically in a straightforward fashion. The recursion relations numerically provide us the phase diagrams in  $(T/J_1, -J_p/J_1, J_{l_1}^{(5)}/J_1)$  space. Let  $T/J_1 = \alpha$ ,  $-J_p/J_1 = \beta$ ,  $J_{l_1}^{(5)}/J_1 = \gamma$  and respectively  $a = \exp(\alpha^{-1})$ ,  $b = \exp(-\alpha^{-1}\beta)$ , and  $c = \exp(\alpha^{-1}\gamma)$ . Starting from the initial conditions

$$x^{(1)} = \frac{b^8 + c^2}{a^2 b^8 c^2 + a^2}, \quad y_1^{(1)} = \frac{b^8 c^2 - 1}{b^8 c^2 + 1}, \quad y_2^{(1)} = \frac{b^8 - c^2}{a^2 b^8 c^2 + a^2},$$

that correspond to the positive boundary condition  $\bar{\sigma}^{(n)}(V \setminus V_n) \equiv 1$ , one iterates the recurrence relations and observes their behavior after a large number of iterations ( $n = 5000$ ). Possible initial conditions with respect to different boundary conditions can be found in [2, 10]. In the simplest situation a fixed point  $(x^*, y_1^*, y_2^*)$  is reached. It corresponds to

FIG. 2: Phase diagrams for  $\gamma = 0$  and  $\beta = 0$ . (Color online)FIG. 3: Phase diagrams for  $\gamma = 1$  and  $\gamma = -1$ .

a *paramagnetic* phase (briefly **P**) if  $y_1^* = 0, y_2^* = 0$  or to a *ferromagnetic* phase (briefly **F**) if  $y_1^*, y_2^* \neq 0$ . The system may be periodic with period  $p$ , i.e., the periodic phase is a configuration with some period. If the case  $p = 2$  corresponds to the *antiferromagnetic* phase (briefly **P2**), then the case  $p = 4$  corresponds to the so-called *antiphase* (briefly **P4**), which is denoted as  $\langle 2 \rangle$  for compactness in [2, 10]. Finally, the system may remain aperiodic. The distinction between a truly aperiodic case and one with a very long period is difficult to make numerically. For detailed information about the phases and the relation with partition functions, we mainly refer to works given by Vannimenus [2], Ganikhodjaev *et al.* [17], and Mariz *et al.* [10]. Below we consider periodic phases with period  $p$  where

FIG. 4: Phase diagrams for  $\gamma = 5$  and  $\gamma = -5$ .FIG. 5: Phase diagrams for  $\beta = 0.2$  and  $\beta = 0.21$ .

$p \leq 12$  (briefly **P2–P12**). We will consider all periodic phases with period  $p > 12$  and aperiodic phases as modulated phases (briefly **M**). A new phase denoted as *paramodulated* found at low temperatures is characterized by zero average magnetization lying inside the modulated phase (for the details see [17]). In the present work we are able to get the complex phase diagrams in the Hamiltonian 3-parameter space. We draw all phase diagrams for the interval  $-2 \leq \alpha, \beta, \gamma \leq 2$ . The resultant phase diagrams for some values of  $\gamma$  and  $\beta$  are shown in Figs. 2–9. All multi-critical points called the *Lifshitz points* are denoted as **LP** and indicated in the complex phase diagrams. We note that the reader is referred to the colored web version of this article. In Fig. 2 for  $\gamma = 0$ , we consider all possible signs of  $J_p$ ,

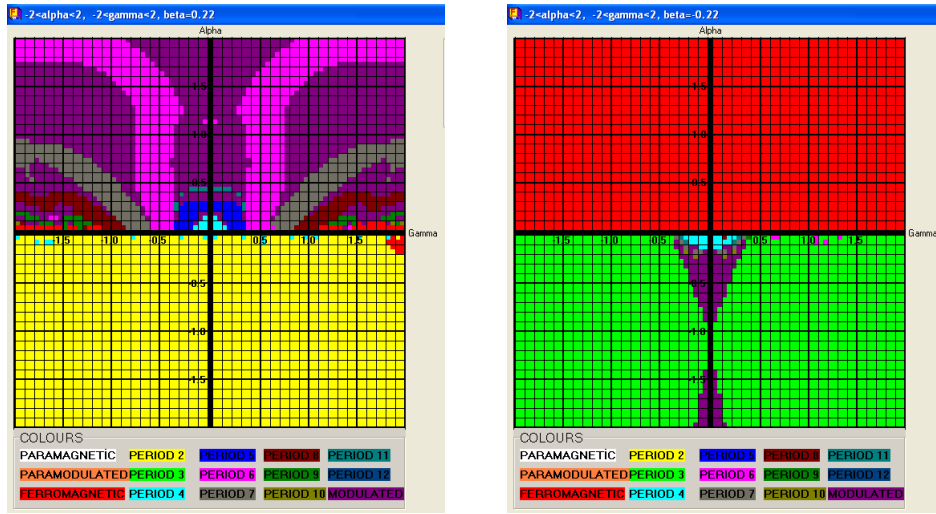


FIG. 6: Phase diagrams for  $\beta = 0.22$  and  $\beta = -0.22$ .

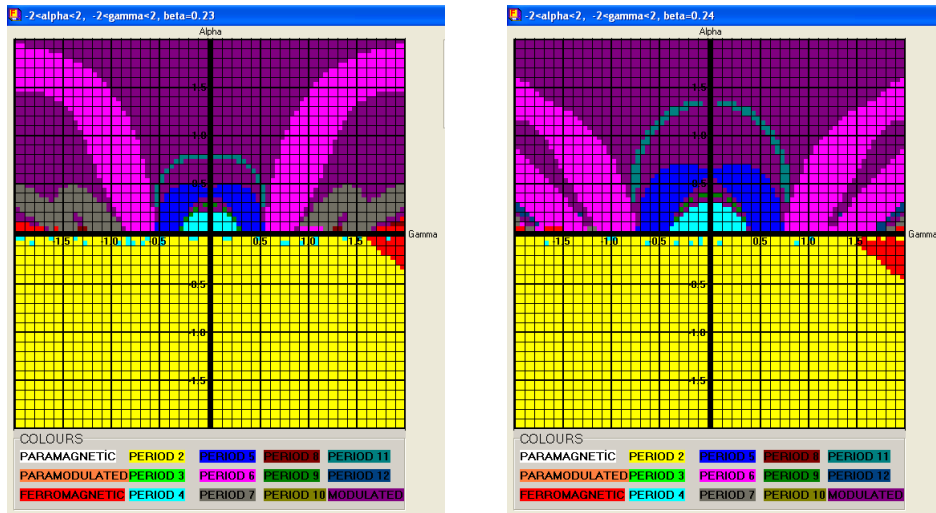


FIG. 7: Phase diagrams for  $\beta = 0.23$  and  $\beta = 0.24$ .

$J_1$ , and  $J_{l_1}^{(5)}$ , whereas in [2] only  $J_1 > 0$  and  $J_p < 0$  were considered. In the first quadrant ( $J_p < 0; J_1 > 0$ ), the phase diagram consists of four phases: **F**, **P**, **M**, and **P4**, three of them (except for **P4**) meeting at the multicritical point ( $T/J_1 = 1.75; -J_p/J_1 = 0.05$ ); we called this point a “three-critical” one, as given in [12, 18]. In the second quadrant ( $J_p > 0; J_1 > 0$ ), the diagram consists of the **F** phase only. Similarly in the fourth quadrant ( $J_p > 0; J_1 < 0$ ) the diagram consists of the **P2** phase only. In the third quadrant ( $J_p > 0; J_1 < 0$ ) the phase diagram consists of mainly the **P4**, **M**, **P**, and **P2** phases. Here three phases, namely the **P2**, **P4**, and **M** phases, meet at the multicritical point ( $T/J_1 = -1.75; -J_p/J_1 = -0.05$ ) that is a three-critical one. An important note is that the phase diagram (Fig. 2) for  $\gamma = 0$

is given in [11] as a Vannimenus extension result on Cayley tree of order  $k = 4$ . In Fig. 2

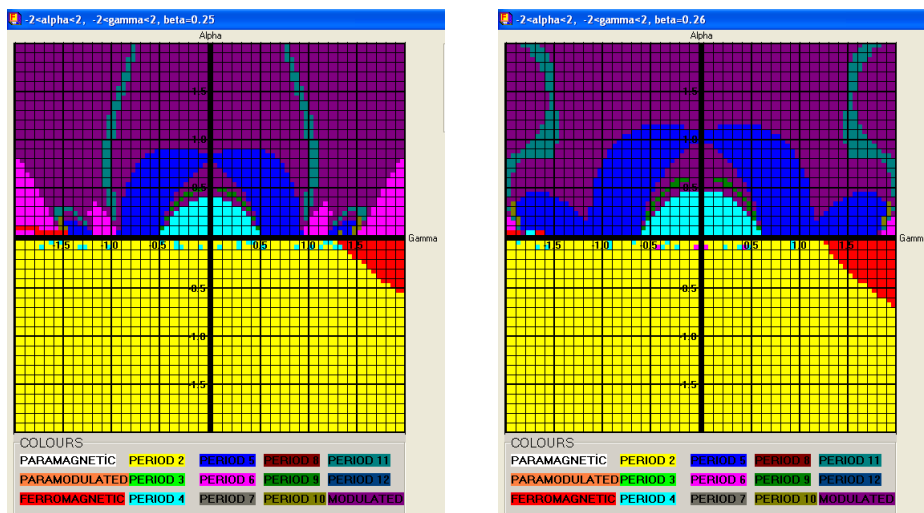


FIG. 8: Phase diagrams for  $\beta = 0.25$  and  $\beta = 0.26$ .

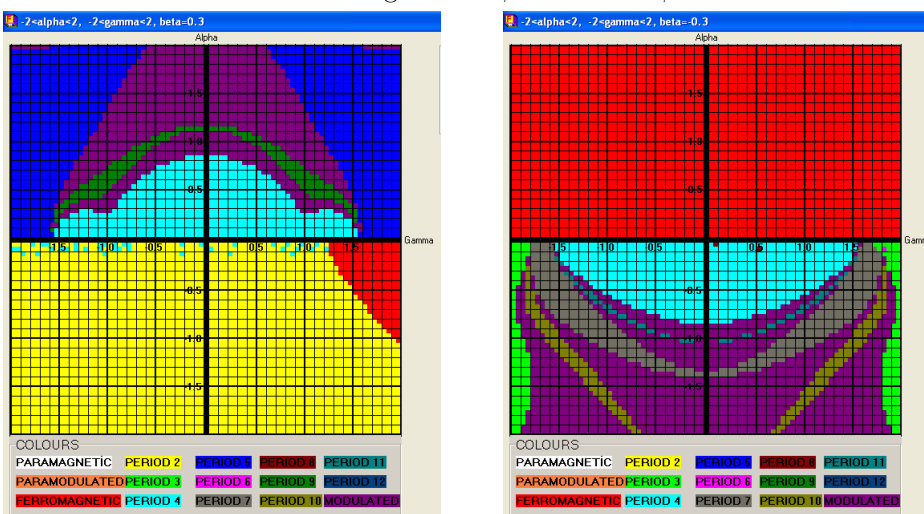


FIG. 9: Phase diagrams for  $\beta = 0.3$  and  $\beta = -0.3$ .

for  $\beta = 0$ , the first and second quadrants ( $J_{l_1}^{(5)}; J_1 > 0$ ) consist of the **F** phase and the third and fourth quadrants ( $J_{l_1}^{(5)}; J_1 < 0$ ) consist of the **P2** phase. In Figs. 3–9, the significance of the parameter  $J_{l_1}^{(5)}$  can be seen. Now in Fig. 3 consider the case  $|J_1| = |J_{l_1}^{(5)}|$ , i.e.,  $|\gamma| = 1$ . For  $\gamma = 1$  the complex phase diagram consists of the **F** and **P2** phases respectively in the second and fourth quadrants. But in the first and third quadrant, some new phases appear in Fig. 3, such as **P3**, **P5**, and **P7**. For  $\gamma = -1$ , similar new phases emerge in the diagrams within the first and third quadrants. In Fig. 4, we consider the case  $|\gamma| = 5$ . In

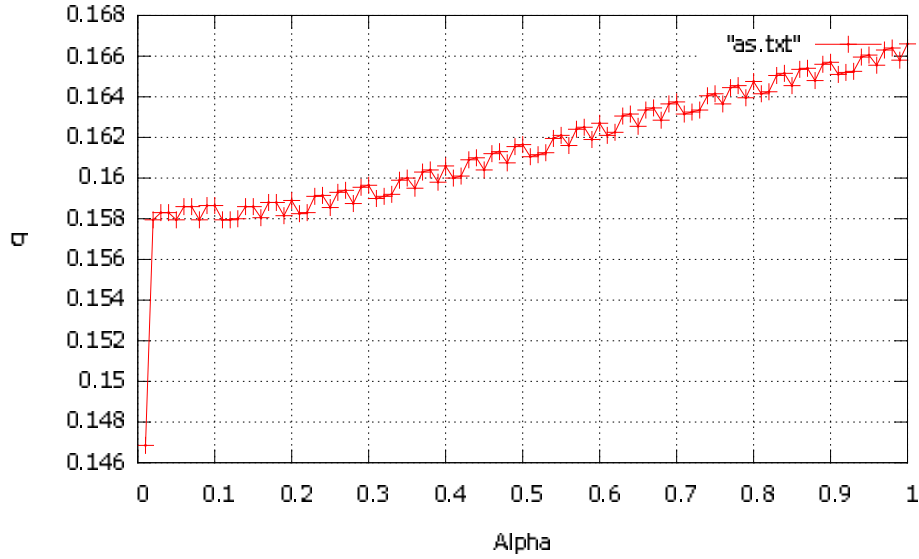


FIG. 10: Variation of the wavevector  $q$  versus temperature for  $\beta = 0.2, \gamma = 0$ .

this diagram, newly appeared phases are growing when  $|\gamma|$  values are increasing, such as **P5** and **P6**. In the next figures (Fig. 5–Fig. 10) we see the significance of the parameter  $J_p$ . Consider the case  $\beta = 0.2$  and  $\beta = 0.21$  (Fig. 5). If  $\beta = 0.2$ , there exists new phases **P7**, **P8**, **P9**, **P10**, and **P11** in the first and second quadrants. If  $\beta = 0.21$ , then **P5** and **P6** also appear in Fig. 5. Also, the phase diagrams consist of some number of islands with different phases. There are some multi-critical points at zero temperature for  $\beta = 0.2$  and  $0.21$ . For the case  $\beta = 0.22$  in Fig. 6, a distinctive feature of the diagram is seen in that the existence of new phases appear as a geometric figures, i.e., the phases with **P5**, **P6**, **P7**, and **P8** in the first and second quadrants. One can see that several multi-critical points exist in the first and second quadrants. If  $\beta = 0.23$  and  $\beta = 0.24$  in Fig. 7, in the first and second quadrants the diagram contains multi-critical points and new phases, phases with **P9** and **P11**. In Fig. 8, there exists some three-critical points: such as  $(T = 0; J_{l_1}^{(5)}/J_1 = \pm 0.5)$  at zero temperature for  $\beta = 0.25$  and  $\beta = 0.26$ . Similarly some new phases emerge in Fig. 9, phases with **P5**, **P9**, and **P11**. There exist also some multi-critical points: such as  $(T/J_1 = 0.2; J_{l_1}^{(5)}/J_1 = 1.55)$  and  $(T/J_1 = 0.2; J_{l_1}^{(5)}/J_1 = -1.55)$  are four-critical points at nonzero temperature in Fig. 9 for  $\beta = 0.3$ . The transition lines between some of the new phases will be considered later on. Also, the phases display chaotic structure [1], which is another subject for the next study.

## V. THE MODULATED PHASE: VARIATION OF THE WAVEVECTOR WITH TEMPERATURE

A question about the modulated phase is: how does the wavevector vary as a function of  $T$  between its value at the ferro-modulated- $\langle 2 \rangle$  transitions and its values in the modulated- $\langle 2 \rangle$  phases? A definition of the wavevector that is convenient for numerical purposes is

$$q = \lim_{N \rightarrow \infty} \left( \frac{1}{2} \frac{n}{N} \right), \quad (4)$$

where  $n$  is the number of times the magnetization (3) changes sign during  $N$  successive iterations. The accurate determination of  $q$  is much easier on a Cayley tree (or Cayley tree-like lattices) than on a periodic lattice, since it is possible to perform several thousand iterations so as to reduce the influence of the initial conditions. For periodic lattices, on the contrary, the boundary conditions introduce rather strong size effects in the numerical studies [2]. Some typical graphs of  $q$  versus  $T$  are drawn in Figs. 10–12 for some  $\gamma$  and  $\beta$  values, slightly near or above the multicritical points (see Figs. 2–4). For Fig. 10, these values ( $\beta = 0.2; \gamma = 0$ ) were chosen because  $q$  is very close to 0.16 at the ferro-modulated transition and a strong locking effect on the simple commensurate structure (+ + + - - -) was expected, as in the ANNNI model [2].

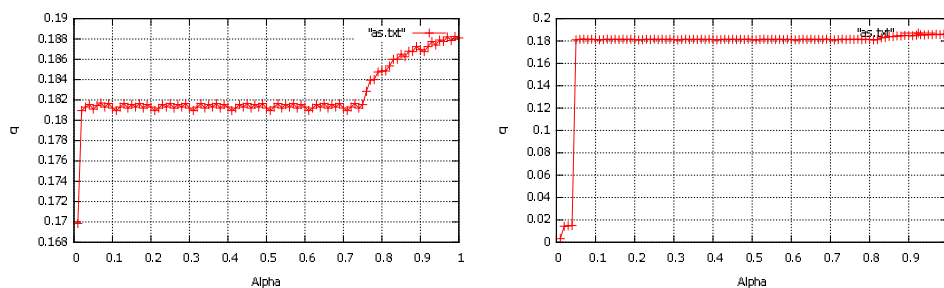


FIG. 11: Variation of the wavevector  $q$  versus temperature for for  $\beta = 0.24, \gamma = 1$  and  $\beta = 0.25, \gamma = 2$  respectively.

At higher temperatures  $q$  goes through a maximum value before reaching its value of 0.18 at the transitions in Fig. 11–Fig. 12. Some interesting features of the curves at the ferro-modulated- $\langle 2 \rangle$  transitions will be discussed in more detail later on.

## VI. CONCLUSIONS

In this paper we have obtained exact phase diagrams of the Ising model with competing prolonged and nearest-neighbor binary interactions, and one-level quinary interactions on a new type of lattice which we called a *Rectangular Chandelier*. We present the variation

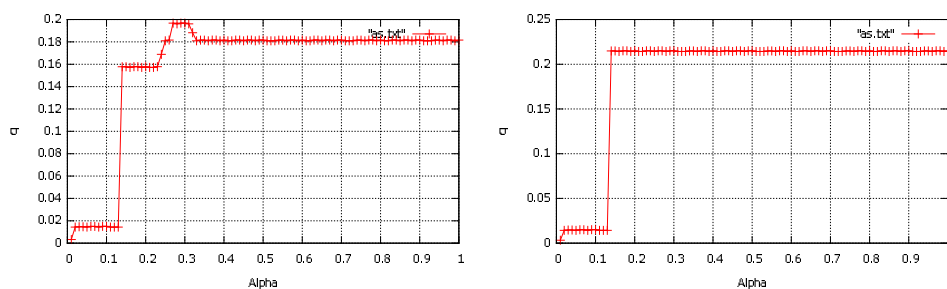


FIG. 12: Variation of the wavevector  $q$  versus temperature for for  $\beta = 0.3, \gamma = 5$  and  $\beta = 0.8, \gamma = 15$  respectively.

of the wavevector with temperature in the modulated phase for some critical points. To understand the role of order  $k$  for the Triangular<sup>( $k=3$ )</sup> and Rectangular<sup>( $k=4$ )</sup> Chandeliers as in the case Cayley tree [11], the same methods can be applied to obtain phase diagrams on a tetragon, pentagon, hexagon, ..., and generally (as we called in [12]) “*Polygon Chandelier*” in future works. Although our models on the Cayley tree-like lattice are very simple, we believe that many of their properties will be reflected in real systems and more realistic models. The study of the Polygon Chandelier with similar methods and models is planned to be the subject of forthcoming publications. To investigate the complex phase diagrams we need to apply some new methods different than linearization. Therefore, the models defined on the Cayley tree-like lattice exhibit quite unusual behaviors. One can see that a distinctive feature of the diagrams is the existence of new phases with interesting geometric figures, namely, phases with **P3**, **P5**, **P6**, **P7**, **P8**, **P9**, and **P11**. The diagrams contain some multicritical Lifshitz points that are at nonzero temperature. It appears that there is a shift of the multicritical Lifshitz point to finite temperature, while such points were stuck at zero temperature  $T$  for all systems with competing interactions, studied on the Cayley tree previously [2, 10]. The other direction of this study can be the analysis of an Ising model on a different type of lattice: a two-layer Bethe lattice with three exchange parameters and in the presence of magnetic fields, which are different in the two layers [15]. Then one could calculate the free energy of that system, and investigate its critical properties, exact phase diagrams, and the shift exponent for the system [16]. Maybe another approach proposed by Inawashiro *et al.* [9] can be applied in our model. Finally the study of additional aspects [13] of this and related models are other subjects for the next publications. In conclusion, we should like to note that the numerical methods presented in this work may be applied to the Potts model [17–19] to obtain the phase diagrams on the Cayley tree-like lattice of order  $k$  ( $k \geq 2$ ). The behavior of the phase diagrams of the Potts model remains of great research interest. Therefore we assume that some new interesting results can be discovered in the phase diagrams of the Potts model in the future.

## Acknowledgements

The authors would like to thank Prof. Dr. N. N. Ganikhodjaev for valuable support and suggestions. We also thank the Editor in-chief and referee(s) for useful suggestions and improvements on the structure of the manuscript.

## References

- \* Electronic address: [hasanakin69@gmail.com](mailto:hasanakin69@gmail.com)  
† Electronic address: [Second.Author@institution.edu](mailto:Second.Author@institution.edu)
- [1] R. F. S. Andrade and S. R. Salinas, *Phys. Rev. E* **56**, 1429 (1997).
  - [2] J. Vannimenus, *Z. Phys. B* **43**, 141 (1981).
  - [3] S. Katsura and M. Takizawa, *Prog. Theor. Phys.* **51**, 82 (1974)
  - [4] T. Hasegawa and K. Nemoto, *Physica A* **387**, 1404 (2008).
  - [5] T. Hasegawa and K. Nemoto, *Physical Review E* **75**, 026105 (2007).
  - [6] J. Rossat-Mignod, P. Burlet, H. Bartholin, O. Vogt, and R. Lagnier, *J. Phys. C: Solid State Phys.* **13**, 6381 (1980).
  - [7] Y. Yamada, I. Shibuya, and S. Hoshino, *Phys. Soc. Japan* **18**, 1594 (1963).
  - [8] S. Inawashiro and C. J. Thompson, *Physics Letters A* **97**, 245 (1983).
  - [9] S. Inawashiro, C. J. Thompson, and G. Honda, *Jour. Stat. Phys.* **33**, 419 (1983).
  - [10] M. Mariz, C. Tsallis, and A. L. Albuquerque, *Jour. Stat. Phys.* **40**, 577 (1985).
  - [11] N. N. Ganikhodjaev, S. Uğuz, S. Temir, and H. Akin, (2010), submitted for publication.
  - [12] S. Uğuz and H. Akin, *Physica A* **389**, 1839 (2010).
  - [13] C. S. O. Yokoi, M. J. Oliveira, and S. R. Salinas, *Phys. Rev. Lett.* **54**, 163 (1985).
  - [14] R. J. Baxter, *Exactly Solved Models in Statistical Mechanics*, (Academic Press, London/New York, 1982).
  - [15] C. Kun Hu, N. Sh. Izmailian, and K. B. Oganesyan, *Phys. Rev. E* **59**, 6489 (1999).
  - [16] P. D. Gujrati, *Phys. Rev. Lett.* **74**, 809 (1995).
  - [17] N. N. Ganikhodjaev, F. Mukhamedov, and C. H. Pah, *Physics Letters A* **373**, 33 (2008).
  - [18] N. N. Ganikhodjaev, S. Temir, and H. Akin, *Jour. Stat. Phys.* **137**, 701 (2009).
  - [19] N. N. Ganikhodjaev, H. Akin, and S. Temir, *Turk. J. Math.* **31**, 229 (2007).